Polymorphism in Halogen-Ethane Derivatives: CCl3-CF2Cl and CF3-CF2Cl

Philippe Négrier, María Barrio, Jose Luis Tamarit, Luis C. Pardo, Denise Mondieig

Polymorphism in Halogen−Ethane Derivatives: CCl_3-CF_2Cl and CF_3-CF_2Cl

Philippe Negrier,[†] María Barrio,[‡] Josep Ll. Tamarit,*[,‡] Luis C. Pardo,[‡] and Denise Mondieig[†]

[†]Université Bordeaux, LOMA, UMR 5798, F-33400 Talence, France, and CNRS, LOMA, UMR 5798, F-33400 Talence, France

[‡]Grup de Caracterització de Materials, Department de Física i Enginyeria Nuclear, ETSEIB, Diagonal 647, Universitat Politècnica de Catalunya, 08028 Barcelona, Catalonia, Spain

ABSTRACT: Molecular crystals of halogen−ethane derivatives $C_2X_{6-n}Y_n$ (X = Cl, Y = F) are known to display order−disorder phase transitions involving changes of the translational, orientational, and conformational order. The appearance of a high-temperature orientationally disordered phase with a high symmetry lattice is expected for this set of compounds in view of their "pseudospherical" molecular geometry. In this work, we present a study of polymorphism of the compounds 1,1,1,2-tetrachloro-2,2-difluoroethane (CCl_3-CF_2Cl) and 1-chloro-1,1,2,2,2-pentafluoroethane (CF_3-CF_2Cl), in which conformational disorder is not present, by combining neutron (D2B and D1B instruments at the Laue-Langevin Institute) and X-ray scattering experiments. We show that despite the close molecular shapes and molecular structures of both compounds, strong differences concerning the disorder appear in the low-temperature phase. The low-temperature phase for CF_3-CF_2Cl is found to be fully ordered, with a monoclinic $P2_1/n$ structure ($Z = 4$), while that of CCl_3-CF_2Cl is found to be orthorhombic *Pmna* ($Z = 4$) with a disorder concerning one Cl and one F sites, each one with a fractional occupancy of 50%. Details related to the high-temperature orientationally disordered phases (both body-centered-cubic) are also given.

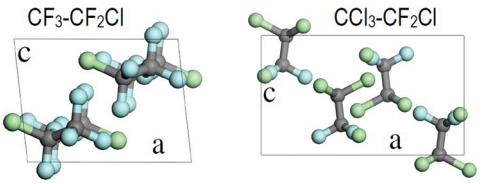

1. INTRODUCTION

Molecular crystals of halogen−ethane derivatives are expected to have order−disorder phase transitions involving changes of the translational, orientational, and conformational orders. Orientational disorder is possible for most of these compounds because of their "pseudospherical" molecular geometry.[1,2] This orientational disorder gives rise to the well-known plastic phases formed by substances whose molecular shapes are symmetrical about one or more axes and, particularly, those where the molecular shape is somewhat globular.[3−7]

Conformational disorder attributed to *trans*−*gauche* transformations is quite usual for compounds of general formula CX_2Y-CX_2Y, where X and Y = F, Cl, Br, or H.[8−16] A common feature of many transitions in organic crystals is the difficulty to achieve the thermal equilibrium between the involved phases, and thus it often leads to the formation of metastable phases that can exist in a wide temperature range.[17] If the disorder existing in a phase, regardless of its nature, is frozen, a "glassy phase" is obtained. This glassy state transforms to the corresponding ergodic phase (i.e., the phase for which the time average and space average for any physical property are identical) on heating at the so-called glass transition temperature, T_g.[6,8,9,18−22]

Although $C_2F_nCl_{6-n}$ compounds have commonly been used as refrigerants, the number of studies about their behavior in the condensed phases is small. The low boiling points of many of these compounds make difficult the study of their polymorphic behavior.

The earliest calorimetric studies of Kolesov et al.[3] and Kishimoto et al.[8] of some isomers with $n = 2$, 3, or 4, namely, CF_2Cl-CF_2Cl, $CF_2Cl-CFCl_2$, and $CFCl_2-CFCl_2$, pointed out the difficulty to obtain a stable solid phase sequence. By cooling their orientational disordered (OD) phase in which mixtures of *trans* and *gauche* conformers are present, both kinds of disorder resulting in a complicated sequence of glass transitions could be trapped. A representative example of this behavior has been described for $CFCl_2-CFCl_2$, for which the existence of two nonequivalent molecular conformations, *trans* with a C_{2h} symmetry and *gauche* with C_2 symmetry, has been claimed as the origin of the difficulty to reach the yet unknown low-temperature ordered phase, for which very partial transformation was obtained after annealing 50 days within a temperature range of the ordered phase.[5,8,16,23,24] Such an effect is accompanied by the two distinct glass transitions, one at 90 K concerning the orientational disorder and an additional one at 130 K related to the freezing in of the ratio between *trans* and *gauche* conformers.

In this work, we present a study of the polymorphic compounds CCl_3-CF_2Cl (the other isomer of the aforementioned $CFCl_2-CFCl_2$) and CF_3-CF_2Cl, which are very close from a molecular point of view. In both molecularly similar compounds, the conformational disorder is not present, so getting the orientationally ordered low-temperature can be achieved. The main thermodynamic properties of the studied compounds are gathered in Table 1. These are, as far as we

Table 1. Temperature Transitions, T_c, and Enthalpy and Entropy Changes Obtained from Available Literature Data for the Different Transitions of CF_3-CF_2Cl and CCl_3-CF_2Cl

compound	transition	T_c, K	ΔH, kJ·mol^{-1}	ΔS J·K^{-1}·mol^{-1}	ref
CF_3-CF_2Cl	II−I	80.24	2.628	32.75	25
	I−L	173.71	1.879	10.82	25
	L−vap	234.04	19.410	82.93	26
CCl_3-CF_2Cl	II−I	158	3.4	21.6	23
	I−L	314.2	3.990	12.7	27
		309.0	3.50	11.3	23
	L−vap	364.7			28

know, the unique results appearing in the literature for these compounds, and they concern exclusively the temperatures and the enthalpy and entropy changes at the ordered to OD phase, the melting of this OD phase, and the vaporization process at normal pressure. We should mention also the work of Pardo et al.[23] concerning the isomers $CFCl_2-CFCl_2$ and CCl_3-CF_2Cl. The authors performed a dynamic study through dielectric relaxation of the OD phases, as well as for the low-temperature phase of CCl_3-CF_2Cl for which, surprisingly, the authors showed the existence of a relaxation process in such a low-temperature phase (<158 K). This relaxation process has a characteristic time of 100 s (i.e., that of a glass transition) at 90 ± 2 K. Complementary specific heat measurements revealed the appearance of a thermal effect reminiscent of that for a glass transition. As the authors pointed out, some kind of disorder, within the temperature domain of the low-temperature phase, should remain in this phase. Similar effects have been found for other plastic crystals in the "ordered" low-temperature phase, such as halogen−methane derivatives,[29−31] adamantanone,[6] and *meta*- and *ortho*-carborane.[32] As for halogen−methane derivatives, the dielectric relaxation process appearing in the low-temperature phases and similar to those appearing in canonical glass formers were explained by the existence of an intrinsic disorder with respect to the occupancy of the halogen (Cl and Br) sites. Large-angle rotations of tetrahedra around the symmetry axes of the molecules produce a statistical occupancy disorder that generates a dipolar moment relaxation.[31,33] At temperatures higher than T_g (i.e., the temperature at which the characteristic time reaches 100 s), the "ordered" phase is ergodic, while at lower temperatures such a disorder is frozen in, and then a nonergodic (glass) state appears. It should be emphasized that the involved compound, CCl_3-CF_2Cl, has no *trans*−*gauche* disorder, so it is interesting to disentangle what kind of disorder can be the cause of the relaxation process.

From a more general point of view, although the systems studied in this work (having translational order) should be subjected to a reduction in the degrees of freedom when compared with canonical glasses (having translational and orientational disorder), the dynamics displays many common features. For this reason, the simple kind of disorder arising from the systems studied in this work concerning low-temperature phases can help to elucidate one of the greatest challenges of condensed matter physics, the glass state.

In this paper, full crystal structure determinations of the low-temperature phases of CF_3-CF_2Cl and CCl_3-CF_2Cl obtained using neutron and X-ray powder diffraction techniques are reported.

2. EXPERIMENTAL SECTION

CCl_3-CF_2Cl and CF_3-CF_2Cl compounds were supplied by ABCR chemical company with purities of 99.9% and 98%, respectively.

The gas sample CF_3-CF_2Cl was cryogenically transferred from the supplier container to the neutron diffraction cell by means of a specially designed system for hydrogen condensation at the Institute Laue-Langevin. The sample CCl_3-CF_2Cl was slowly heated just above the melting point and handled under controlled atmosphere to the neutron sample container and to the Lindemann capillary for the X-ray diffraction measurements.

2.1. Neutron Diffraction Measurements. Neutron powder diffraction patterns of CF_3-CF_2Cl were collected at 10 K (low-temperature phase) and 140 K (high-temperature OD phase) using the high-resolution D2B instrument at ILL (Grenoble).[34] Data were collected using wavelength λ = 2.398 Å in a 2θ-range from 20° to 160° with a step size of 0.05°. High-resolution data from the equatorial detector bank were utilized for the Rietveld refinement.

The crystallographic structure of CCl_3-CF_2Cl was studied by combining the neutron and X-ray diffraction. Neutron powder diffraction measurements were performed by means of D1b high-intensity powder diffractometer at the ILL (λ = 2.52 Å) equipped with an 80° position-sensitive detector at 5 and 125 K. The recorded 2θ-range was from 10° to 120° with a step size of 0.2°.

2.2. High-Resolution X-ray Powder Diffraction Measurements. High-resolution X-ray powder diffraction patterns of CCl_3-CF_2Cl were recorded by means of a horizontally mounted INEL cylindrical position-sensitive detector (CPS120) equipped with a liquid nitrogen 700-series cryosystem cooler from Oxford Cryosystems (temperature accuracy of 0.1 K), which enabled isothermal measurement in the 100−300 K range.

The detector was used in the Debye−Scherrer geometry (transmission mode), enabling a simultaneous recording of the profile over a 2θ-range between 4° and 120° (angular step of 0.029° in 2θ). Monochromatic Cu Kα_1 radiation (λ = 1.5406 Å) was selected with asymmetric focusing incident-beam curved graphite monochromator. External calibration was performed by using $Na_2Ca_2Al_2F_{14}$.[35,36]

The samples were introduced in Lindemann capillaries (0.3-mm diameter), which rotated perpendicularly to the X-ray beam during the experiment to minimize possible effects of preferred orientations.

2.3. Density Measurements. Density measurements at normal pressure in the liquid state of CCl_3-CF_2Cl from the melting point to 350 K were carried out using an Anton Paar D5000 densimeter with temperature stability of ±0.02 K, giving rise to uncertainties in density of ca. 5×10^{-5} g·cm^{-3}. The densimeter was calibrated as described in ref 30.

3. RESULTS AND DATA ANALYSIS

3.1. Structure Determination of the Low-Temperature Phases. Indexing of the neutron and X-ray powder diffraction patterns, structure solutions, and Pawley and Rietveld refinements were performed using Materials Studio Program.[37]

3.1.1. CF_3-CF_2Cl. X-Cell software[38] available in the module Powder Indexing of Materials Studio was used to index as monoclinic the neutron powder diffraction pattern of the CF_3-CF_2Cl obtained at 10 K in the D2B diffractometer after pseudo-Voigt fitting of the Bragg peaks. Once indexing was complete, the systematic absences to determine the most likely space groups were compatible to the space group $P2_1/n$, and Z = 4 was assigned for a reasonable density.

Taking advantage of the existence of a unique molecular conformation, a rigid body molecule was built up by means of the software Forcite from Materials Studio package together with the Compass forcefield.[37] Bond distances and angles according to the minimization energy process converged to the values gathered in Table 2.

Pawley refinement was carried out using the initial unit-cell parameters in space group $P2_1/n$. The unit-cell parameters,

Table 2. Intramolecular Bond Lengths (Å) and Angles (deg) of the CF_3−CF_2Cl and CCl_3−CF_2Cl Rigid Molecules Obtained Using the Forcite Software from Materials Studio[a]

molecule	CF_3−CF_2Cl	CCl_3−CCl_3	CCl_3−CF_2Cl
C1−C2	1.537	1.584	1.529
C1−Cl(i)		1.767−1.771	1.779−1.780
C1−F(i)	1.339−1.345		1.342
C2−Cl(i)	1.771	1.771−1.779	1.772
C1−C2−F(i)	112.5		110.77
C1−C2−Cl(i)	111.4−111.5	109.7−109.8	112.47
C2−C1−Cl(i)		109.5−109.7	110.1−110.7
Cl(i)−C1−Cl(i)		109.2−109.7	108.3−108.6
F(i)−C1−F(i)	107.0 − 107.5		
F(i)−C2−F(i)	106.5		106.8
F(i)−C2−Cl(i)	107.8 − 107.98		107.9

[a]For the sake of comparison, values of the low-temperature orthorhombic phase of CCl_3−CCl_3 from Hohlwein et al.[39] are enclosed.

zero-point shift, background, peak profile (pseudo-Voigt), and peak asymmetry parameters were refined. The constructed molecule was then placed in a general position within the unit cell, and the module Powder Solve was used to solve the structure. In the final Rietveld refinement, the position and orientation of the molecule was refined with the rigid-body constraint and with a single overall isotropic displacement parameter. All of the profile parameters referred to above were also refined, and preferred orientation was fitted using the Rietveld−Toraya function.[40]

The final Rietveld calculated profile and the experimental one are shown in Figure 1 together with the difference between

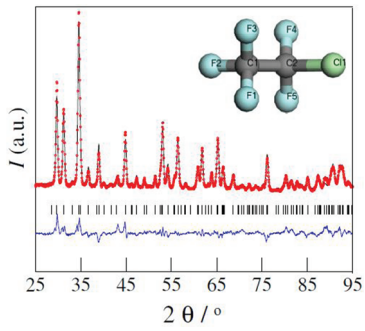

Figure 1. Experimental (red circles) and calculated (black line) neutron diffraction patterns along with the difference profile (blue line) and Bragg reflections (vertical sticks) of $P2_1/n$ monoclinic phase II of CF_3−CF_2Cl (at 10 K). Inset corresponds to the rigid molecule according to the minimization energy.

them and Bragg reflections. The parameters refined in the procedure are gathered in Table 3 and the coordinates of the atoms of the asymmetric unit are collected in Table 4.

3.1.2. CCl_3−CF_2Cl. Similar procedures were used to solve the structure of CCl_3−CF_2Cl by means of the high-resolution X-ray powder diffraction pattern at 100 K. After indexing, systematic absences were found to verify those of the *Pnma* and $Pna2_1$ (with permutation between *b* and *c* parameters) space groups. In general, such space groups contain $Z = 8$ and $Z = 4$, respectively. For CCl_3−CF_2Cl, we have $Z = 4$ according to the reasonable density values. So the first attempt was made with the $Pna2_1$ group. The result clearly showed the molecule on the mirror existing in the *Pnma* space group with one fluorine atom on it. Due to the molecular symmetry, the molecular mirror must relate both F atoms and, consequently, Cl atoms attached to the same C atom. This implies that Cl and the last F atoms are disordered. With this constraint, the molecule was placed on the aforementioned mirror.

In addition, the final structure was refined by means of a Rietveld procedure by assuming one F atom and one Cl atom being disordered, with site occupancy factors for them of 0.5. The structure was confirmed by an independent Rietveld procedure performed with the neutron diffraction pattern (D1b instrument) at 5 K. Figure 2 displays the results of X-ray and neutron Rietveld refinement. Table 3 gathers the refined parameters and Table 5 the fractional coordinates for the structure at 100 K derived from X-ray diffraction.

3.2. Lattice Symmetry of the High-Temperature Orientationally Disordered Phases. Due to the orientational disorder, structural analysis was restricted to a Pawley profile-fitting procedure.

3.2.1. CF_3−CF_2Cl. The neutron powder diffraction pattern at 140 K obtained with D2B diffractometer was coherently indexed according to a body-centered-cubic (bcc) lattice with a cell constant of 6.454 Å. Such a symmetry lattice makes the OD phase of this compound isostructural to other members of the halogen−ethane series, such as the well studied CCl_2F−CCl_2F.[8,14]

3.2.2. CCl_3−CF_2Cl. The lattice symmetry of the OD high-temperature phase of this compound was previously reported[8,24] as bcc with a probable space group $Im\bar{3}m$ as for C_2Cl_6.[41] Our X-ray measurements as a function of temperature from the II−I transition temperature to the melting point confirm such previous result. The cubic lattice parameter at 170 K was determined to be 7.024(2) Å.

3.3. Lattice Parameter As a Function of Temperature. X-ray powder diffraction experiments were performed on heating from 100 K up to the melting temperature for CCl_3−CF_2Cl to determine the volume changes at the II−I and melting phase transitions, as well as the thermal expansion tensor.

The refined lattice parameters and unit cell volume were fitted by a standard least-squares method as a function of temperature. The polynomials describing the temperature variation of both phases II and I are shown in Table 6, while the molar volume as a function of temperature, enclosing that of the liquid state obtained from density measurements, is plotted in Figure 3. Such a figure shows that the molar volumes determined by means of neutron powder diffraction at 5 and 125 K perfectly match the fitted curve. (See Supporting Information for the lattice parameters of phases II and I as a function of temperature). Volume changes at the II−I and I−L transitions were determined to be 3.90 and 10.19 $cm^3 \cdot mol^{-1}$, respectively. It can be seen that despite the OD character of phase I, the volume change at the melting process is more than 2.5 that of the II−I transition. Similar examples can be found for other plastic phases when the same kind of disorder is present in the phase below the plastic phase.[30,42−45]

4. DISCUSSION

The monoclinic ($P2_1/n$) lattice structure of the low-temperature phase of CF_3−CF_2Cl at 10 K contains four molecules per unit cell, the asymmetric unit being one molecule. Figure 4 shows several projections along different crystallographic planes of this structure and the lattice parameters at 10 K are reported in Table 3. The molecules stack in sheets along the *ac* plane, with the C−C intramolecular direction tilted alternately with respect to the *b* direction. As can be seen in Table 7, the

Table 3. Results from the Rietveld Refinement of the Low-Temperature Phases II of CF_3-CF_2Cl and CCl_3-CF_2Cl

chemical formula	CF_3-CF_2Cl	CCl_3-CF_2Cl	CCl_3-CF_2Cl
M, g·mol^{-1}	154.466	203.830	203.830
2θ angular range	20 - 160 °	25 − 120°	15 − 80°
space group	$P2_1/n$	*Pnma*	*Pnma*
a, Å	7.0283 ± 0.0004	10.6015 ± 0.0016	10.6877 ± 0.0012
b, Å	12.5494 ± 0.0006	9. 5857 ± 0.0012	9.6604 ± 0.0008
c, Å	5.2893 ± 0.0004	6.2179 ± 0.0008	6.2379 ± 0.0005
β, deg	96.432 ± 0.005		
V/Z, Å^3	115.9	157.97	160.98
Z (Z')	4 (1)	4(1)	4(1)
temp	10 K	5 K	100 K
D_x, g·cm^{-3}	2.213	2.142	2.103
radiation type, λ	neutron, λ = 2.398 Å	neutron, λ = 2.52 Å	X-ray, λ = 1.5406 Å
2θ shift (zero correction)	−0.0629 ± 0.0024	0.280 ± 0.005	−0.0006 ± 0.0021
profile parameters			
Na	0.268 ± 0.015	0.266 ± 0.022	0.000 ± 0.020
reliability parameters			
R_{wp}	6.89%	3.86%	2.84%
R_p	5.22%	2.98%	2.17%
peak width parameters			
U	0.326 ± 0.020	2.41 ± 0.16	0.662 ± 0.107
V	0.017 ± 0.030	−0.72 ± 0.15	0.134 ± 0.056
W	0.177 ± 0.010	0.21 ± 0.03	0.017 ± 0.007
overall isotropic temperature factor, U, Å^2	0.0173 ± 0.0005	0.0213 ± 0.0009	0.0199 ± 0.001
preferred orientation (Rietveld−Toraya function)			
a*	0.22891	0.06162	−0.90095
b*	0.97326	0.00000	−0.09341
c*	−0.01930	0.99810	0.42376
G2	0.32159	0.62994	0.87934
G1	0.19657	0.84819	0.96185

Table 4. Fractional Coordinates of the Low-Temperature Phase II of CF_3-CF_2Cl at 10 K

atom	X	Y	Z
C1	0.6869(4)	0.9103(2)	0.7263(7)
C2	0.8547(4)	0.8352(2)	0.8111(6)
Cl1	1.0647(3)	0.8725(4)	0.6767(8)
F1	0.6458(6)	0.9105(3)	0.4720(7)
F2	0.5268(4)	0.8834(2)	0.8262(9)
F3	0.7298(4)	1.0110(2)	0.7967(8)
F4	0.8958(5)	0.8350(4)	1.0655(6)
F5	0.8136(4)	0.7340(2)	0.7427(11)

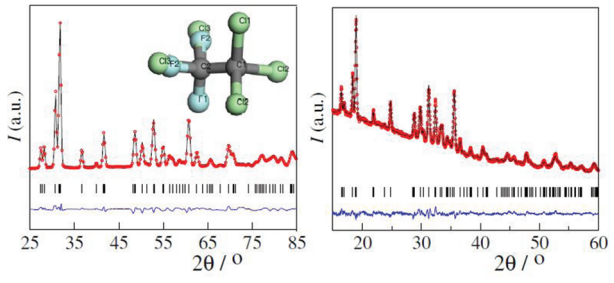

Figure 2. Experimental (red circles) and calculated (black line) neutron (left panel) at 5 K and X-ray (right panel) at 100 K diffraction patterns along with the difference profile (blue line) of *Pnma* orthorhombic phase II of CCl_3-CF_2Cl. Inset corresponds to the rigid molecule according to the energy minimization.

shortest intermolecular F···F distance is 2.820 Å, appearing along the b direction between alternative ($h0l$) planes, is very close to the van der Waals radius of the F atom.[46] These close contacts associated with the high electronegativity of the F atom give rise to a dense packing of this compound.

Table 5. Fractional Coordinates of the Low-Temperature Phase II of CCl_3-CF_2Cl at 100 K

atom	X	Y	Z	fractional occupancy
C1	0.3770(2)	0.2500	0.4964(4)	1.0
C2	0.3946(2)	0.2500	0.2531(4)	1.0
Cl1	0.5247(2)	0.2500	0.6283(4)	1.0
Cl2	0.2925(2)	0.1005(0)	0.5792(4)	1.0
Cl3	0.4807(2)	0.1039(0)	0.1613(4)	0.5
F1	0.2837(2)	0.2500	0.1528(4)	1.0
F2	0.4551(2)	0.3642(0)	0.1891(4)	0.5

As for the low-temperature structure of CCl_3-CF_2Cl, the most striking fact is the occupational disorder between F2 and Cl3, with equal occupational factor of 0.5. Such a disorder produces a dipole fluctuation that is the cause of the dielectric relaxation measured previously in this compound.[23] The authors wrote "... some disorder remains in phase II which freezes at 90 K". In fact, the present work demonstrates that below the transition temperature between phases II and I at 158 K, there is not a structural change until the lowest temperature reached in this study (5 K), and thus the specific heat anomaly detected previously at 90 K is due to the freezing (at a time scale of 100 s) of the F and Cl occupational disorder. Otherwise, at temperatures lower than 90 K, the orthorhombic phase becomes nonergodic from a dynamical point of view. A similar effect has been reported for some halogen−methane derivatives (CBr_nCl_{4-n}) in which the disorder concerns the

Table 6. Polynomial Equations $p = p_0 + p_1T + p_2T^2$ (T in K and p in Å) to Which the Lattice Parameters of CCl_3-CF_2Cl Were Fitted As a Function of Temperature and Molar Volume (v in $cm^3 \cdot mol^{-1}$), R, the Reliability Factor Defined as $R^2 = \sum[p_{exp} - p_c]^2/p_c^2$), Where p_{exp} and p_c Are the Measured and Calculated Lattice Parameters, Respectively, and a Two-Parameter Polynomial Equation for the Molar Volume (v) of the Liquid State

phase	temperature range, K	parameter	p_0	$p_1 \times 10^3$	$p_2 \times 10^5$	$R \times 10^3$
II	100–158	a, Å	10.64(10)	0.65(17)	1.09(65)	0.100
		b, Å	9.613(41)	−0.429(65)	0.82(25)	0.011
		c, Å	6.105(29)	1.88(47)	−0.55(18)	0.008
I	160–305	a, Å	6.735(19)	1.67(17)	0.017(40)	0.014
L	310–350	v, $cm^3 \cdot mol^{-1}$	74.16(9)	166.3(3)		46

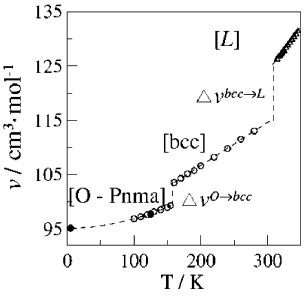

Figure 3. Molar volume for the orthorhombic (O), body-centered-cubic (bcc), and liquid (L) phases of CCl_3-CF_2Cl as a function of temperature from X-ray (○), neutron diffraction (●), and densitometry (△) measurements.

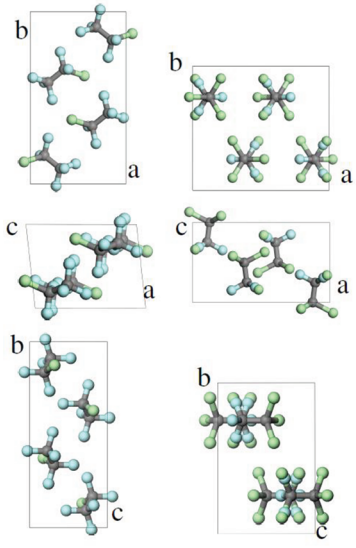

Figure 4. Projection of the $P2_1/n$ and *Pnma* structures of phases II of CF_3-CF_2Cl (left row) and CCl_3-CF_2Cl (right row) in the (00l) (top), (0k0) (middle), and (h00) (bottom) planes. Cl green; F blue; C gray.

Br and Cl atoms within the low-temperature monoclinic structure.[31]

As for the structural details of the orthorhombic *Pnma* structure of CCl_3-CF_2Cl, close similarities with that of the low-temperature orthorhombic phase of C_2Cl_6 (also *Pnma*) emerge. In fact, the occupational disorder present in the structure of CCl_3-CF_2Cl simulates a C_{2v} symmetry (F1 sites on the mirror plane) from a dynamical point of view, making the arrangement of the molecules in the lattice completely similar to low-temperature orthorhombic phase of C_2Cl_6. In both cases, the C–C bonds are parallel to the (0k0) plane, the molecules being alternatively tilted with respect to the [00l] direction an angle

Table 7. Selected Shortest Intermolecular Distances (in Å)[a]

molecule	CF_3-CF_2Cl, T = 10 K	CCl_3-CF_2Cl, T = 5 K	CCl_3-CCl_3, T = 140 K
C–C···C–C	4.980	5.501	5.897
Cl···Cl	3.766	3.504	3.619
Cl···F	3.319	3.178	
F···F	2.820	3.790	

[a]C–C···C–C stands for the middle of the C–C bond of the molecule) The shortest F···F distance within the disordered structure of CCl_3-CF_2Cl is given for the F·· F2 and F···Cl_3, due to the F2–Cl3 occupational disorder (see Table 5). Data for CCl_3-CCl_3 are calculated from Hohlwein et al.[39]

of 7.0° (125 K) and 6.7° (5 K) in CCl_3-CF_2Cl and 12.5° in C_2Cl_6 (at 140 K).[39]

An indication of how strong the F···F electrostatic interaction is in the low-temperature phase of CF_3-CF_2Cl is given by the packing coefficient. This packing coefficient is defined as $\eta = V_m/(V/Z)$, in which V_m is the van der Waals volume of the molecule (115.9 $Å^3$ for CF_3-CF_2Cl and 160.98 $Å^3$ for CCl_3-CF_2Cl) and V/Z is the volume occupied by a molecule in the lattice. The calculated packing coefficients are 0.747 (at 10 K) and 0.736 (at 5 K) for CF_3-CF_2Cl and CCl_3-CF_2Cl, respectively. Disregarding the temperature difference, the F···F interaction seems to put closer the molecules within the ordered monoclinic structure of CF_3-CF_2Cl. These figures go along the distances between molecules, which are considerably shorter for molecules containing fluorine atoms (see Table 7).

The influence of the occupational disorder on the intermolecular interactions has been studied by means of the isobaric thermal expansion tensor. The principal axes of the isobaric thermal expansion tensor allows determination of the directions of the weakest and highest deformation (commonly referred to as hard and soft directions, respectively) related to the directions of the corresponding intermolecular interactions in the crystal structure.[44,47]

For an orthorhombic lattice, according to the Newmann's principle (for which the thermal-expansion tensor has to display the point group symmetries of the crystal), the principal directions are coincident with the lattice axes of the crystal.

Figure 5 shows the variation of the principal coefficients of the thermal expansion tensor as a function of temperature. For this variation, it can be seen that the hardest direction (i.e., the lowest deformation due to a temperature change) for the whole temperature range of phase II corresponds to the c direction, while the (00l) planes contain the soft directions. This result also emerges by a simple inspection of the three-dimensional plots of the isobaric thermal expansion tensor for this phase presented in Figure 6. According to the lattice structure (see Figure 4), it can be seen that the hardest direction is close to the C–C orientation of the molecules

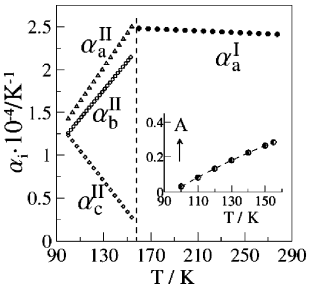

Figure 5. Variation of the principal coefficients of the thermal expansion in phase II (ergodic region) and phase I. Inset shows the aspherism index in the ergodic region of phase II of CCl_3–CF_2Cl.

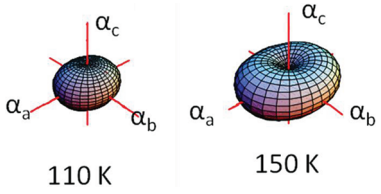

Figure 6. Thermal expansion tensors at 110 K (left) and 150 K (right) of phase II of CCl_3–CF_2Cl.

(alternatively tilted around 7° with respect to the *c* axis) and, due to the occupational disorder, parallel to the molecular dipoles. In other words, the occupational disorder gives rise to a dynamical disorder, which makes possible the time-average orientation of the dipoles along the *c* direction, and thus a strong dipole–dipole interaction along such direction. Very similar results were found in the low-temperature phases of *tert*-butyl molecules ($(CH_3)_3CX$, X = CN, Cl, Br) for which the rotations along the dipole axis (C'_3-rotations) make hard the interactions along the dipolar axis and soft within the planes perpendicular to those axes.[42] The fact that the (00*l*) planes become softer and softer with the increase of temperature coherently agrees with the increase of the dipolar reorientational frequency as previously stated.[23]

This strong anisotropy is accounted by means of the aspherism index, defined as $A = {}^2/_3[1 - (3\beta/\alpha_v^2)^{1/2}]$, where $\beta = \alpha_1\alpha_2 + \alpha_2\alpha_3 + \alpha_1\alpha_3$, and $\alpha_V = (1/v)(\partial v/\partial T)_P = \sum_{i=1}^{3} \alpha_i$ is the volume expansivity.[48] The inset in Figure 5 shows that the aspherism index increases with increasing temperature and thus anisotropy increases (for an isotropic, that is, cubic phase, $A = 0$). This means that with increasing temperature the dipole fluctuations due to the occupational site disorder will gain in amplitude, making softer the interactions between molecules within the (00*l*) planes. The 3D-plot of the thermal expansion tensor at 150 K (Figure 6) enhances this result.

As far as the thermal expansion of the OD phase I is concerned, it reaches a high value due to overall tumbling of the molecules.

5. CONCLUSIONS

The polymorphic behavior of CF_3–CF_2Cl and CCl_3–CF_2Cl has been studied from low temperature to the liquid state. The low-temperature structure of CF_3–CF_2Cl has been found to be monoclinic $P2_1/n$ ($Z = 4$) at 10 K, while the high-temperature orientationally disordered phase has been indexed as body-centered-cubic, both of them characterized by means of neutron powder diffraction.

As for the low-temperature phase II of CCl_3–CF_2Cl, the orthorhombic *Pnma* ($Z = 4$) structure reveals the existence of occupational disorder between one F and one Cl atom. Such a disorder explains the origin of the previously found dipole orientational disorder, which gives rise to a significant relaxation process.[23] The high-temperature solid phase for this compound displays also body-centered-cubic symmetry, thus being isostructural to that of C_2Cl_6 compound. Results from neutron and X-ray powder diffraction were found to be in perfect agreement.

As far as we know, this work describes the first structures of fully halogenated ethane derivatives (Freon compounds). These compounds have a great number of applications in refrigeration systems despite the impact of these molecules on the ozone layer and thus their contribution to the global warning.[49] It is surprising that the solid-state properties of these materials have not previously been studied in detail.

AUTHOR INFORMATION

Corresponding Author

*E-mail: jose.luis.tamarit@upc.edu.

ACKNOWLEDGMENTS

This work was supported by the Spanish Ministry of Science and Innovation (Grant FIS2011-24439) and the Catalan Government (Grant 2009SGR-1251). We thank the technical service at the ILL Institute for its support with the measurements and C. Cabrillo for supplying us the experimental setup for in situ gas condensation of CF_3–CF_2Cl on the D2B sample holder.

REFERENCES

(1) Powell, B. M.; Press, W.; Dolling, G.; Sears, V. F. *Mol. Phys.* **1984**, *53*, 941.
(2) Parsonage, N. G.; Staveley, L. A. K. *Disorder in Crystals*; Clarendon: Oxford, 1978.
(3) Kolesov, V. P.; Kosarukina, E. A.; Zhogin, D. Yu.; Poloznikova, M. E.; Pentin, Yu. A. *J. Chem. Thermodynamics* **1981**, *13*, 115.
(4) Reuter, J.; Büsing, D.; Tamarit, J. Ll.; Würflinger, A. *J. Mater. Chem.* **1997**, *7*, 41.
(5) Rovira-Esteva, M.; Murugan, N. A.; Pardo, L. C.; Busch, S.; Tamarit, J. Ll.; Cuello, G. J.; Bermejo, F. J. *Phys. Rev. B* **2011**, *84*, No. 064202.
(6) Brand, R.; Lunkenheimer, P.; Loidl, A. *J. Chem. Phys.* **2002**, *116*, 10386.
(7) Pardo, L. C.; Veglio, N.; Bermejo, F. J.; Tamarit, J.Ll.; Cuello, G. J. *Phys. Rev. B* **2005**, *72*, No. 014206.
(8) Kishimoto, K.; Suga, H.; Seki, S. *Bull. Chem. Soc. Jpn.* **1978**, *51* (6), 1691.
(9) Angell, C. A.; Dworking, A.; Figuiere, P.; Fuchs, A.; Szwarc, H. *J. Chim. Phys. Phys.-Chim. Biol.* **1985**, *82*, 773.
(10) Iwasaki, M.; Nagase, S.; Kojima, R. *Bull. Chem. Soc. Jpn.* **1957**, *30*, 230.
(11) Pethrick, R. A.; Wyn-Jones, E. *J. Chem. Soc. A* **1971**, *1*, 54.
(12) Kagarise, R. E.; Daasch, L. W. *J. Chem. Phys.* **1955**, *23*, 113.
(13) Newmark, R. A.; Sederholm, C. H. *J. Chem. Phys.* **1965**, *42*, 602.
(14) Krüger, J. K.; Schreiber, J.; Jiménez, R.; Bohn, K.-P.; Smutný, F.; Kubát, M.; Petzelt, J.; Hrabovské-Bradshaw, J.; Kamba, S.; Legrand, J. F. *J. Phys.: Condens. Matter* **1944**, *6*, 6947.
(15) Affouard, F.; Descamps, M. *Phys. Rev. E* **2005**, *72*, No. 012501.
(16) Sharapova, I. V.; Krivchikov, A. I.; Korolyuk, O. A.; Jezowski, A.; Rovira-Esteva, M.; Tamarit, J. Ll.; Pardo, L. C.; Ruiz-Martin, M. D.; Bermejo, F. J. *Phys. Rev. B* **2010**, *81*, No. 094205.
(17) Pardo, L. C.; Barrio, M.; Tamarit, J. Ll.; López, D. O.; Salud, J.; Negrier, P.; Mondieig, D. *Phys. Chem. Chem. Phys.* **2001**, *3*, 2644.

(18) Angell, C. A.; Ngai, K. L.; McKenna, G. B.; McMillan, P. F.; Martin, S. W. *J. Appl. Phys.* **2000**, *88*, 3113.
(19) Puertas, R.; Rute, M. A.; Salud, J.; López, D. O.; Diez, S.; van Miltenburg, J. C.; Pardo, L. C.; Tamarit, J. Ll.; Barrio, M.; Pérez-Jubindo, M. A.; de la Fuente, M. R. *Phys. Rev. B* **2004**, *69*, No. 224202.
(20) Drozd-Rzoska, A.; Rzoska, S. J.; Pawlus, S.; Tamarit, J. Ll. *Phys. Rev. B* **2006**, *73*, No. 224205.
(21) Romanini, M.; Martinez-Garcia, J. C.; Tamarit, J. Ll.; Rzoska, S. J.; Barrio, M.; Pardo, L. C.; Drozd-Rzoska, A. *J. Chem. Phys.* **2009**, *131*, No. 184504.
(22) Martinez-Garcia, J. C.; Tamarit, J. Ll.; Capaccioli, S.; Barrio, M.; Veglio, N.; Pardo, L. C. *J. Chem. Phys.* **2010**, *132*, No. 164516.
(23) Pardo, L. C.; Lunkenheimer, P.; Loidl, A. *J. Chem. Phys.* **2006**, *124*, No. 124911.
(24) Pardo, L. C.; Bermejo, F. J.; Tamarit, J. Ll.; Cuello, G. J.; Lunkenheimer, P.; Loidl, A. *J. Non-Cryst. Solids* **2007**, *353*, 999.
(25) Aston, J. G.; Wills, P. E.; Zolki, T. P. *J. Am. Chem. Soc.* **1955**, *77*, 3939.
(26) Domalski, E. S.; Hearing, E. D. *J. Phys. Chem. Ref. Data* **1996**, *25*, 1.
(27) Golovanova, Yu.G.; Kolesov, V. P. *Vestn. Mosk Univ., Ser. 2: Khim.* **1984**, *25*, 244.
(28) *CRC Handbook of Data on Organic Compounds*, 2nd ed.; Weast, R. C., Grasselli, J. G., Eds.; CRC Press, Inc.: Boca Raton, FL, 1989; p 1.
(29) Barrio, M.; Tamarit, J. Ll.; Negrier, Ph.; Pardo, L. C.; Veglio, N.; Mondieig, D. *New J. Chem.* **2008**, *32*, 232.
(30) Parat, B.; Pardo, L. C.; Barrio, M.; Tamarit, J. Ll.; Negrier, Ph.; Salud, J.; López, D. O.; Mondieig, D. *Chem. Mater.* **2005**, *17*, 3359.
(31) Zuriaga, M.; Pardo, L. C.; Lunkenheimer, P.; Tamarit, J. Ll.; Veglio, N.; Barrio, M.; Bermejo, F. J.; Loidl, A. *Phys. Rev. Lett.* **2009**, *103*, No. 075701.
(32) Lunkenheimer, P.; Loidl, A. *J. Chem. Phys.* **1996**, *104*, 4324.
(33) Zuriaga, M.; Carignano, M.; Serra, P. *J. Chem. Phys.* **2011**, *135*, No. 044504.
(34) Hewat, A. W. *Phys. B: Condens. Matter* **2006**, *385*−*86*, 979.
(35) Ballon, J.; Comparat, V.; Pouxe, J. *Nucl. Instrum. Methods* **1983**, *217*, 213.
(36) Evain, M.; Deniard, P.; Jouanneaux, A.; Brec, R. *J. Appl. Crystallogr.* **1993**, *26*, 563.
(37) MS Modeling (Material Studio) version 4.1: http://www.accelrys.com /mstudio/ms_modeling.
(38) Neumann, M. A. *J. Appl. Crystallogr.* **2003**, *36*, 356.
(39) Hohlwein, D.; Nägele, W.; Prandl, W. *Acta Crystallogr.* **1979**, *B35*, 2975.
(40) Toraya, H.; Marumo, F. *Mineral. J.* **1981**, *10*, 211. Rietveld, H. M. *J. Appl. Crystallogr.* **1969**, *2*, 65.
(41) Gerlach, P.; Hohlwein, D.; Prandl, W.; Schulz, F. N. *Acta Crystallogr.* **1981**, *A37*, 904.
(42) Negrier, Ph.; Barrio, M.; Tamarit, J. Ll.; Veglio, N.; Mondieig, D. *Cryst. Growth Des* **2010**, *10*, 2793.
(43) Jenau, M.; Reuter, J.; Tamarit, J. Ll.; Würflinger, A. *J. Chem. Soc., Faraday Trans.* **1996**, *92*, 1899.
(44) Tamarit, J. Ll.; López, D. O.; Alcobé, X.; Barrio, M.; Salud, J.; Pardo, L. C. *Chem. Mater.* **2000**, *12*, 555.
(45) Barrio, M.; de Oliveira, P.; Céolin, R.; López, D. O.; Tamarit, J. Ll. *Chem. Mater.* **2002**, *14*, 851.
(46) Kirsch, P. *Modern Fluoroorganic Chemistry: Synthesis, Reactivity, Applications*; Wiley-VCH Verlag GmbH&Co. KgaA: Weinheim, Germany, 2004.
(47) Salud, J.; Barrio, M.; López, D. O.; Alcobe, X.; Tamarit, J. Ll. *J. Appl. Crystallogr.* **1998**, *31*, 748.
(48) Weigel, D.; Beguemsi, T.; Garnier, P.; Gerad, J. F. *J. Solid State Chem.* **1978**, *23*, 241.
(49) Wosfy, S. C.; McElroy, M. B.; Sze, N. C. *Science* **1975**, *187*, 535.